UDK 669.715:620.18
Original scientific article/Izvirni znanstveni članek

ISSN 1580-2949
MTAEC9, 41(6)283(2007)

MICROSTRUCTURAL EVALUATION OF RAPIDLY SOLIDIFIED Al–7Cr MELT SPUN RIBBONS

OVREDNOTENJE MIKROSTRUKTURE HITROSTRJENIH TRAKOV Al-7Cr

Peter Jurči[1], Mária Dománková[2], Mária Hudáková[2], Borivoj Šuštaršič[3]

[1]ECOSOND, Ltd., K Vodárně 531, 257 22 Čerčany, Czech Republic
[2]STU Trnava, J. Bottu 52, 917 24 Trnava, Slovak Republic
[3]IMT, Lepi pot 11, 1000 Ljubljana, Slovenia
p.jurci@seznam.cz

Prejem rokopisa – received: 2007-09-20; sprejem za objavo – accepted for publication: 2007-10-18

The use of conventional bulk materials is limited by segregation phenomena, which are generated during the solidification and cannot be eliminated in the solid state. The introduction of rapid-solidification technology (RST) into material processing overcame some of the problems of unacceptable material quality and broadened the range of materials that it is possible to fabricate.
The use of conventional ingot metallurgy for the fabrication of aluminium alloys containing a large amount of elements with a low diffusion coefficient is impossible because coarse, hard and brittle intermetallics are formed and the alloys have poor mechanical properties. The use of RST makes it possible to produce these alloys with an improved microstructure; however, before industrial production the structure and properties of the rapidly solidified semi-products as well as the consolidated bulk product must be evaluated systematically.
In this paper, melt-spun ribbons, made under various conditions from a binary Al–7%Cr, alloy are investigated. The structure consisted of a supersaturated Al solid solution with a high dislocation density, precipitates of chromium-rich phases and rosette-like spherolites formed from the Al solid solution and the Al_7Cr intermetallic phase. The type of phases is related to the processing conditions in only a very limited way.

Keywords: rapid solidification, melt spinning, ribbons, microstructure

Praktična uporaba konvencionalnih kovinskih materialov je omejena zaradi izcejanja zlitinskih elementov. To nastaja zaradi različnih vzrokov in pojavov med strjevanjem in ga je praktično nemogoče odpraviti s kasnejšo toplotno obdelavo v trdnem stanju. Hitro strjevanje in njegova vpeljava kot tehnologije za procesiranje različnih kovinskih materialov premaguje to oviro in razširja izbiro materialov.
Uporaba konvencionalne metalurgije ingotov za izdelavo Al zlitin z velikim deležem legirnih elementov z majhnim difuzijskim koeficientom je praktično nemogoča, ker v mikrostrukturi nastajajo grobi delci trdih in krhkih intermetalnih spojin in imajo zlitine nizke mehanske lastnosti. Uporaba tehnologije hitrega strjevanja omogoča izdelavo teh zlitin z izboljšano mikrostrukturo, pred vpeljavo te tehnologije v redno proizvodnjo pa je treba sistematično analizirati strukturo in lastnosti hitrostrjenih polproizvodov ter iz njih izdelanega zgoščenega izdelka.
V tem članku obravnavamo raziskave hitro strjenih trakov zlitine Al z masnim deležem Cr 7 %, izdelanih pri različnih pogojih. Preiskave so pokazale, da mikrostrukturo sestavljajo: s Cr prenasičena trdna raztopina Al z veliko gostoto dislokacij ter izločki na Cr bogatih faz, kakor tudi peritektik v obliki rozet nastal iz trne raztopine Al in intermetalne faze Al_7Cr. Ugotovili smo, da je oblika in velikost posameznih faz relativno malo odvisna od izbranih pogojev izdelave hitro strjenih trakov.

Ključne besede: hitro strjevanje, nalivanje na hitrovrteči se valj, trakovi, mikrostruktura

1 FUNDAMENTAL

The industrial use of metallic materials is limited by their microstructure and mechanical properties, characteristics that are greatly influenced by the initial casting operation. During slow cooling in large industrial ingots a considerable amount of segregation takes place due to the different solubilities in the solid and the liquid, and this cannot be improved via a solid-state thermal treatment. Only a rapid solidification can successfully overcome the problems connected with segregation and produce fine-grained, segregation-free materials with an unusual chemical composition and unique mechanical properties.

Rapidly solidified (RS) materials differ a great deal from materials with the same chemical composition prepared by conventional casting procedures in terms of the refinement of the main structural constituents [1–3]. As a result of non-equilibrium freezing, they may also contain supersaturated phases, metastable intermediate phases or, in limited cases, amorphous constituents [4,5]. The results affect the microstructures and the properties of materials, in many cases favourably, and this positive effect of RS on materials' characteristics has been clearly determined [6–8].

One typical example where the rapid solidification is required to obtain material with acceptable properties is the group of aluminium alloys with elements that have a negligible solid solubility and a low diffusion coefficient. In conventionally produced Al alloys, elements like Fe, Ni, V, Cr, etc. are considered as impurities, since they form coarse and brittle aluminides. On the other hand, Al alloys containing elements with a low diffusion coefficient made by the RS technique exhibit an

excellent combination of toughness and elongation and are stable up to relatively high temperatures [7,8].

The Al–Cr system is a very typical example. The solid solubility of chromium in aluminium is very low. In slowly solidified material, for example, chromium forms large needle-like as well as branch-like particles of Al_xCr_y intermetallics, which have a deleterious effect on the mechanical properties. On the other hand, powder-metallurgy materials based on this binary system, with the addition of some other elements, can easily achieve an ultimate tensile strength up to 600 MPa during an elongation of several percents [9,10].

2 EXPERIMENTAL

The Al_7Cr alloy was prepared from technically pure aluminium and chromium. The mixture made from raw materials was molten in a vacuum furnace and overheated up to 1150 °C in order to eliminate the occurrence of large and hardly soluble intermetallics in the melt.

Melt-spun ribbons were prepared in an experimental device, i.e., the Melt-Spinner M-10, in IMT, Ljubljana. The metals were melted under an argon overpressure. The rotation speed of the copper wheel ranged between 900 r/s and 1350 r/s (16.8 ms^{-1} and 25.2 ms^{-1}). Other important parameters of the melt-spinning process are given in **Table 1**.

The microstructure of the alloy was investigated using light microscopy (slowly solidified material) and transmission electron microscopy (melt-spun ribbons). The microstructure of the slowly solidified material was revealed by using the Dix-Keller reagent. Thin foils were prepared directly from the rapidly solidified ribbons using a TENUPOL 2® device. A mixture of 30 % nitric acid and 70 % methanol was used as an etching agent. The thinning was carried out at a temperature of –30 °C and a bias of 19 V.

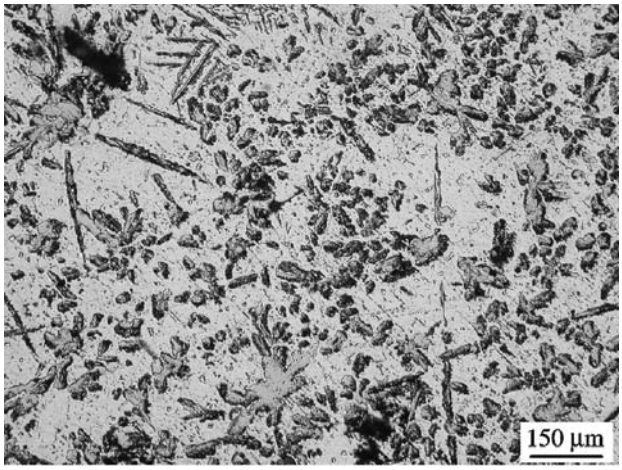

Figure 1: Optical micrograph of the slowly solidified alloy with star-shaped formations of intermetallics

Slika 1: Optični posnetek počasi strjene zlitine z zvezdastimi intermetalnimi spojinami

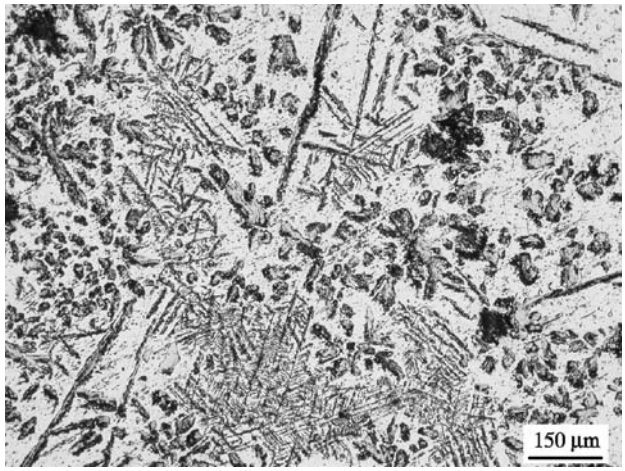

Figure 2: Optical micrograph of the slowly solidified alloy with semi-globular particles of intermetallics

Slika 2: Optični posnetek počasi strjene zlitine s polkroglastimi intermetalnimi spojinami

3 RESULTS AND DISCUSSION

The microstructure of the slowly solidified material in an as-cast ingot is shown in **Figures 1 and 2**. **Figure 1** shows an optical micrograph of the slowly solidified alloy with star-shaped formations of intermetallics, and **Figure 2** shows the slowly solidified alloy with semi-globular particles of intermetallics.

The alloy has a dendritic solidification morphology composed of a relatively large amount of intermetallic phases, which differ from each other mainly in shape and size. Some of them have a globular, convex shape, which indicates primary crystallization from the melt. In some cases, star-shaped formations are found in the micro-

Table 1: Important parameters of the melt spinning process

Tabela 1: Pomebni parametri procesa hitrega strjevanja

Sample designation	Superheating of the melt	Induction heating power	Atmosphere (vacuum + Ar 5.9)	Wheel speed	Nozzle diameter
	°C			m/s	mm
Al-1	1030	3 kW to 500 °C 7 kW to 1030 °C (heating rate approx. 70 °C/min.)	60 kPa overpressure of argon	16.8	2.2
Al-2				19.6	0.8
Al-3				25.2	0.8

structure, **Figure 1**. Their occurrence can be related to the primary crystallization and a peritectic reaction between the intermetallic and the Al solid solution.

From the binary Al–Cr equilibrium diagram only the Al_7Cr intermetallic would be expected for our chosen composition, although with an increased Cr content other compounds would also be possible ($Al_{11}Cr_2$, Al_4Cr, Al_3Cr, Al_9Cr_4, etc.) [11,18]. All these intermetallics are non-stoichiometric compounds (Bertholides) with a relatively narrow range of possible compositions.

X-ray diffraction fixed the Al solid solution with sharp diffraction lines. This indicates that during a slow solidification no supersaturation of the solid solution occurred, **Figures 3 and 4**. The second phase was identified as the $Al_{13}Cr_2$ compound, **Figure 3**. In the binary diagram reported in [11] there is only the isoconcentration Al_7Cr phase. In reference [12], it is suggested that the phase is stable in a given concentration range. Taking into account the fact that the investigated alloy has a lower chromium content than the compound, the stoichiometry $Al_{13}Cr_2$ may correspond to the lower limit of the range for the Al_7Cr compound. In addition, an intermetallic phase with the same stoichiometry was also found by Selke [13] in the bulk alloy Al–15 % Cr. In this alloy the chromium content is also below the concentration range of the phase Al_7Cr [12]; it is, however, twice as high as in the alloy investigated in this work. Pearson´s Handbook also mentions the $Al_{45}Cr_7$ phase. The stoichiometric ratio of 45:7 is between that of 13:2 and 7:1 and, with respect to the actual chemical composition of the alloy, the probability of its occurrence is lower than that for the $Al_{13}Cr_2$. Therefore, identifying this intermetallic as $Al_{13}Cr_2$ is considered to be correct.

Figure 5 shows one of the features of the specimen Al-1. This type is represented by a primary crystallized rosette-like particle having a size of about 250 nm. Electron diffraction patterns fixed this phase as $Al_{11}Cr_2$ aluminide, in good agreement with the Al–Cr binary equilibrium diagram [12], where the $Al_{11}Cr_2$ phase is in

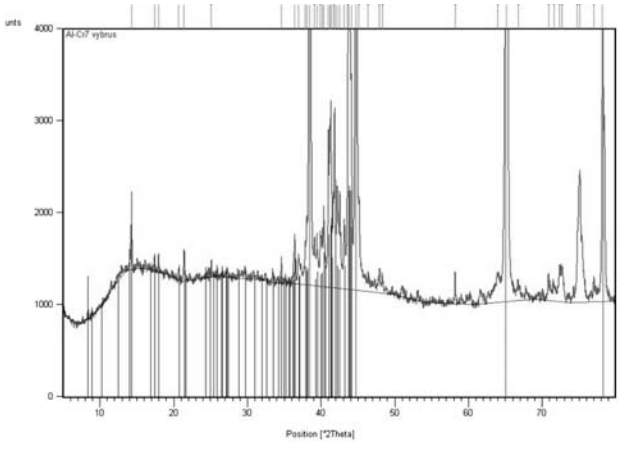

Figure 3: X-ray patterns from the slowly solidified material: red lines, Al; blue lines, $Al_{13}Cr_2$

Slika 3: Rentgenska difrakcijska slika počasi strjene zlitine: Al – rdeče črte, $Al_{13}Cr_2$ – modre črte

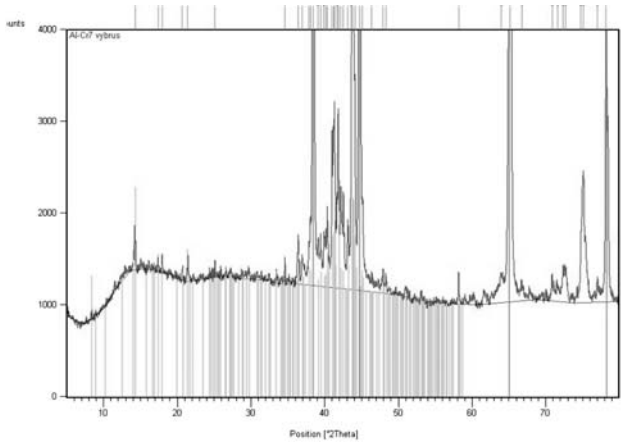

Figure 4: X-ray patterns from the slowly solidified material: red lines, Al; green lines, $Al_{45}Cr_7$

Slika 4: Rentgenska difrakcijska slika počasi strjene zlitine: Al – rdeče črte, $Al_{45}Cr_7$ – zelene črte

equilibrium with the residual melt above 785 °C. In the slowly solidified alloy, the $Al_{11}Cr_2$ phase decomposes normally to the Al solid solution with a negligible Cr content and the phase Al_7Cr. However, if the solidification rate is rapid enough the phase can be conserved in the alloy down to room temperature.

Figure 6 shows the aluminium solid-solution matrix with a relatively high dislocation density in the same specimen. The electron diffraction patterns revealed a

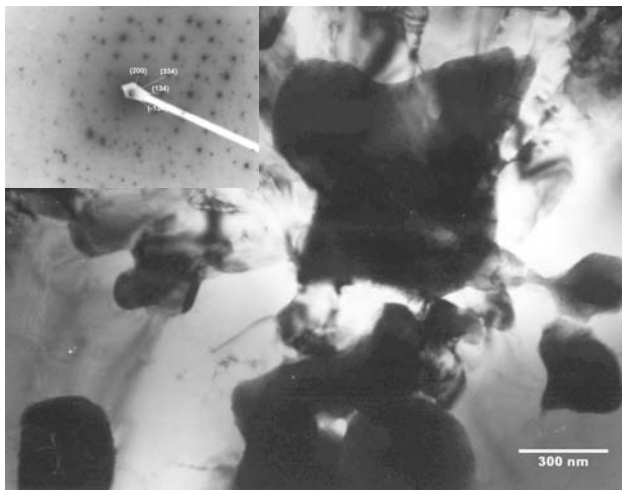

Measured values		Tabular values for the $Al_{11}Cr_2$	
č.s.	$d_{vyp}/(10^{-10}\,m)$	(h k l)	$d_{hkl}/(10^{-10}\,m)$
1	6.25	2 0 0	6.17
2	4.35	1 3 4	4.30
3	3.10	3 3 4	3.06
4	4.35	–1 3 4	4.30
$\varphi_{1/2} = 69°$		$\varphi_{(200)a(134)} = 69.6°$	

Figure 5: A typical primary particle in the specimen Al-1

Slika 5: Značilen primarni delec v vzorcu Al-1

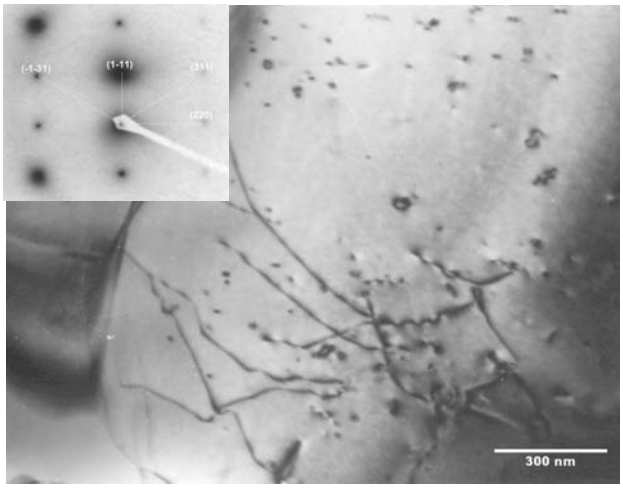

Measured values		Tabular values for the (Al)	
č.s.	$d_{vyp}/(10^{-10}m)$	(h k l)	$d_{hkl}/(10^{-10}m)$
1	2.43	1 -1 1	2.34
2	1.48	2 2 0	1.43
3	1.26	3 1 1	1.22
4	1.26	-1 -3 1	1.22
$\varphi_{1/2} = 90°$		$\varphi_{(1\text{-}11)a(220)} = 90°$	

Figure 6: The Al solid-solution matrix in the specimen Al-1
Slika 6: Matica trdne raztopine v vzorcu Al-1

lattice distortion in comparison to the equilibrium situation. Both of these phenomena can be ascribed to the rapid solidification, which produced the supersaturation of the solid solution and the enhanced dislocation density in the matrix.

The TEM micrograph in **Figure 7** shows the rosette-like spherolite from the sample Al-2. The circular-shaped constituent with a diameter of 2 μm consists of the Al solid solution and an intermetallic phase, identified as the Al_4Cr aluminide.

Figure 8 shows the second constituent, which consists of many semi-globular particles with a size of several tens of nanometers, surrounded by dislocation clusters. These particles correspond very well to the high-temperature δ-phase with a stoichiometry of Al_9Cr_4. The matrix is formed in a similar way as in the previous specimen from the supersaturated Al solid solution.

The last constituent of the microstructure of the investigated melt-spun ribbons is presented in **Figure 9**. It consists of vermicular Al_7Cr precipitates embedded in the Al solid-solution matrix. As confirmed by the electron diffraction, the lattice spacings do not correspond exactly to the equilibrium Al_7Cr phase; they are smaller, which suggests that the phase is also partly non-equilibrium.

To understand the nature of the phases occurring in thin melt-spun ribbons, the Al–Cr equilibrium diagrams [11,12] must first be taken into consideration. Shunk [14] reported that θ-$Al_{13}Cr_2$ and η-$Al_{11}Cr_2$ are the equilibrium

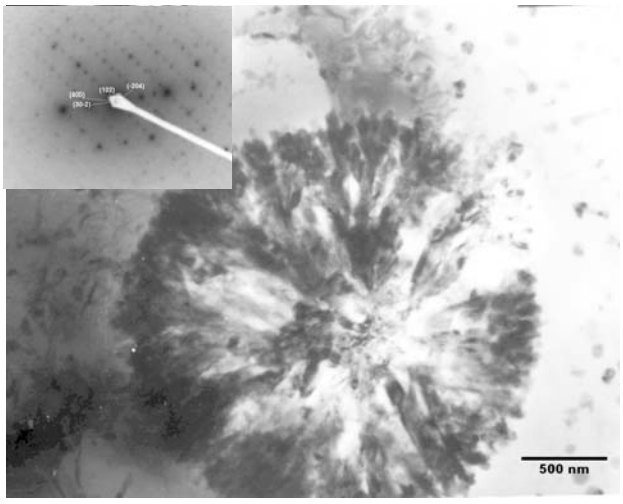

Measured values		Tabular values for the Al_4Cr	
č.s.	$d_{vyp}/(10^{-10}m)$	(h k l)	$d_{hkl}/(10^{-10}m)$
1	10.43	1 0 2	10.10
2	5.35	3 0 -2	5.25
3	4.40	4 0 0	4.34
4	5.13	-2 0 4	5.05
$\varphi_{1/2} = 80°$		$\varphi_{(102)a(30\text{-}2)} = 79.5°$	

Figure 7: Rosette-like spherolite in the specimen Al-2
Slika 7: Rozetasti sferoliti v vzorcu Al-2

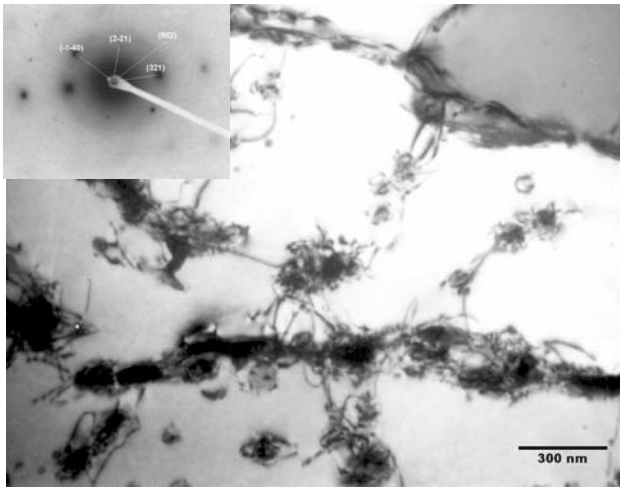

Measured values		Tabular values for the Al_9Cr_4	
č.s.	$d_{vyp}/(10^{-10}m)$	(h k l)	$d_{hkl}/(10^{-10}m)$
1	3.04	2 -2 1	3.04
2	2.43	3 2 1	2.43
3	1.64	5 0 2	1.69
4	2.27	-1 -4 0	2.21
$\varphi_{1/2} = 72°$		$\varphi_{(2\text{-}21)a(321)} = 74.5°$	

Figure 8: Semi-globular particles in the Al matrix in the specimen Al-2
Slika 8: Polglobularni delci v aluminijevi matici v vzorcu Al-2

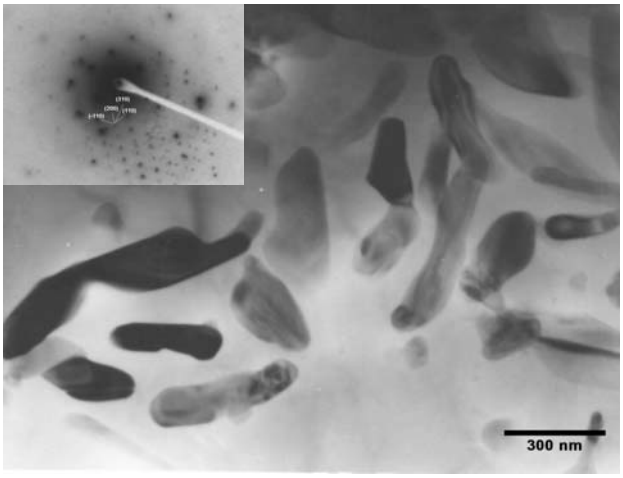

Measured values		Tabular values for the Al_7Cr	
Č.s.	$d_{vyp}/(10^{-10}m)$	(h k l)	$d_{hkl}/(10^{-10}m)$
1	9.20	2 0 0	9.83
2	6.85	1 1 0	7.06
3	4.45	3 1 0	4.95
4	6.85	-1 1 0	7.06
$\varphi_{1/2} = 74°$		$\varphi_{(200)a(110)} = 72.8°$	

Figure 9: The Al_7Cr precipitates in the specimen Al-3
Slika 9: Izločki Al_7Cr v vzorcu Al-3

phases for the pure Al–Cr system. However, at a higher concentration the $Al_{11}Cr_2$ phase is present at room temperature in the diagram [12], and only above 790 °C can this phase be expected to be an equilibrium aluminide in the alloy. However, it is expected to occur in the melt-spun ribbon, either as a direct consequence of the normal solidification or as a result of non-equilibrium freezing.

There is no unequivocal information concerning the Al_7Cr aluminide. In a diagram in [11], the Al_7Cr phase is shown as an isoconcentric intermetallic compound. On the other hand, the phase is shown in [12] to occur in some narrow concentration range. The stoichiometry 13:2 is slightly smaller that 7:1; thus, θ-$Al_{13}Cr_2$ can probably be considered as a chromium-poor variant (Bertholide) of the Al_7Cr aluminide.

Other phases with a higher chromium content (Al_4Cr, Al_9Cr_4) can be expected at room temperature only after slow solidification in the alloys with a high chromium content. At temperatures above 940 °C (Al_4Cr) and 1030 °C (Al_9Cr_4) the occurrence of both phases is also shifted to a lower chromium content.

During investigations of alloy processing, theories relating to the structure of the melt were suggested. For instance, it was determined that the structure of the solid alloy is in many cases also conserved to a limited extent in the liquid as a constituent with short-range order. The constituents with long-range orders of atoms were described as clusters on the basis of the "clusters theory" [15-17]. It is important that these clusters often have the same compositions as the nearest solid phase. In the rapidly solidified alloy the clusters (or the phases with a similar chemical composition) can be conserved to room temperature, and this is the principal explanation for their occurrence in the ribbons.

In addition, Selke [13] suggested that an "i-phase" occurred in the splat-quenched $Al_{85-x}Cu_xCr_{15}$ alloys; however, no information about its stoichiometry for the pure Al–Cr system was found so far. Therefore, it is practically impossible to estimate whether it corresponds to the identified phases in the Al–7%Cr alloy or not.

4 CONCLUSIONS

The microstructure of the slowly solidified alloy Al–7% Cr consists of the matrix, primary globular or semi-globular dendrites and intermetallic phases. The matrix is an Al solid solution and the intermetallic phases are mainly the compound Al_7Cr ($Al_{13}Cr_2$).

The microstructure of RS ribbons consists of the matrix with a high dislocation density and of nano-crystalline phases of different size, shape and distribution. The matrix is a supersaturated solid solution in which many different phases occur. Some of them are semi-equilibrium, while the Al_9Cr_4 and Al_4Cr phases are of a non-equilibrium origin. The RS ribbons processed by various conditions differ from each other mainly in terms of the quantity and the occurrence of non-equilibrium phases.

5 REFERENCES

[1] Tewari, S. N.: J. Mater. Sci. Lett. 11 (**1992**), 1020–1022
[2] Muller, B. A., Tanner, L. E., Perepezko, J. H.: Mater. Sci. Eng. A150 (**1992**), 123–132
[3] Zhang, X., Atrens, A.: Mater. Sci. Eng. A159 (**1992**), 243–251
[4] Era, H., Kishitake, K., Li, P.: Metall. Trans., 24A, (**1993**) 3, 751–756
[5] Kuoji, M. et al.: J. Mater. Sci. 29 (**1994**), 1449–1454
[6] Jurči, P.: PhD Thesis, MtF STU Trnava, 1996 (In Czech)
[7] Ehrstrom, J. C., Ponesu, A.: Mater. Sci. Engng., A186 (**1994**), 55–64
[8] Premkumar, M. K., Lawley, A., Koczak, M. J.: Mater. Sci. Engng., A174 (**1994**), 127–139
[9] Jones, H.: Mater. Sci. Engng., A375-377 (**2004**), 104–111
[10] Lieblich, M. et al.: Mater. Sci. Techn., 12 (**1996**), 25–33
[11] Web page: http://aluminium.matter.org.uk/content/html/eng/default.asp?catid=79&pageid=-884660481
[12] Smithells Metal Reference Book, 8th Edition, Elsevier, 2004
[13] Selke, H., Ryder, P. L.: Mater. Sci. Engng., A165 (**1993**), 81–87
[14] Shunk, I. A.: Constitution of Binary Alloys, Second Supplement, McGraw-Hill, New York, 1969
[15] Stewart, G. W., Benz, C. A.: Phys. Rev., 46 (**1934**), 703
[16] Frenkel, Ja. I.: Kinetic theory of liquids, Leningrad, 1975 (In Russian)
[17] Danilov, V. I., Rabčenko, I.V.: ŽETF 7, 1937, 1153 (In Russian)
[18] M. Hansen, K. Anderko: Constitution of binary diagrams, 1958